applied sciences

MDPI

Article

Deep Inorganic Fraction Characterization of PM_{10}, $PM_{2.5}$, and PM_1 in an Industrial Area Located in Central Italy by Means of Instrumental Neutron Activation Analysis

Maurizio Manigrasso [1], Geraldo Capannesi [2], Alberto Rosada [2], Monica Lammardo [3], Paolo Ceci [4], Andrea Petrucci [5] and Pasquale Avino [6,*]

1 Department of Technological Innovations, INAIL, via IV Novembre 144, I-00187 Rome, Italy; m.manigrasso@inail.it
2 ENEA, R.C.-Casaccia, via Anguillarese 301, I-00060 Rome, Italy; geraldocapannesi@gmail.com (G.C.); albertorosada@libero.it (A.R.)
3 FSN-FISS-RNR, ENEA, R.C.-Casaccia, via Anguillarese 301, I-00060 Rome, Italy; monica.lammardo@enea.it
4 CNR, Institute of Atmospheric Pollution Research, Division of Rome, c/o Ministry of Environment, Land and the Sea, via Cristoforo Colombo 44, I-00147 Rome, Italy; ceci@iia.cnr.it
5 INMRI, ENEA, R.C.-Casaccia, via Anguillarese 301, I-00060 Rome, Italy; andrea.petrucci@enea.it
6 Department of Agriculture, Environment and Food Sciences (DiAAA), University of Molise, via F. De Sanctis, I-86100 Campobasso, Italy
* Correspondence: avino@unimol.it; Tel.: +39-0874-404-631

Received: 10 March 2020; Accepted: 1 April 2020; Published: 7 April 2020

Abstract: Atmospheric pollution is an important task in life sciences and, in particular, inorganic fraction characterization is considered as an important issue in this field. For many years, researchers have focused their attention on the particulate matter fraction below 10 μm: in this case, our attention was also focused on $PM_{2.5}$ (i.e., particles with a size fraction smaller than 2.5 μm) and PM_1 (below 1 μm). This paper would like to investigate whether the element accumulation in different granulometric fractions is similar, or whether there are behavior dissimilarities. Among the different analytical techniques, the instrumental neutron activation analysis, an instrumental nuclear method, was used for its peculiarity of investigating the sample without performing any chemical-physical treatment. Forty-two daily samples using the reference method were collected, 15 filters for PM_{10}, 18 for $PM_{2.5}$, and 12 for PM_1; the filters, along with primary standards and appropriate standard reference materials, were irradiated at the National Agency for New Technologies, Energy and Sustainable Economic Development (ENEA) R.C.-Casaccia's Triga MARK II reactor. The irradiations carried out in the Rabbit and Lazy Susan channels allowed for the investigation of 36 elements and the relative Pearson's correlations between elements and PM-fractions (PM_{10} vs. $PM_{2.5}$ was good, whereas PM_{10} vs. PM_1 was the worst). The Enrichment Factors were studied for the three fractions to show how anthropogenic sources have affected the element content. A comparison between these data and element levels determined worldwide showed that our concentrations were lower than those determined in similar scenarios. Furthermore, a statistical approach (source discrimination, hierarchical cluster analysis, principal component analysis) has allowed us to identify similarities between the samples: the airborne filters can be divided in two main groups (i.e., one made of PM_{10} and $PM_{2.5}$ filters and one only of PM_1 filters), meaning a different element contribution to this fraction coming from other sources present at the site.

Keywords: inorganic fraction; incineration plant; PM fractions; PM_1; INAA; EFs; source discrimination; multivariate analysis

1. Introduction

Atmospheric pollution is a relevant task in life sciences and, in particular, inorganic fraction characterization is considered an important issue in this field. For many years, researchers have focused their attention on the particulate matter fraction below 10 μm: nowadays, general attention has been focused on $PM_{2.5}$ (i.e., particles below 2.5 μm) and PM_1 (below 1 μm). In previous papers [1,2], the authors investigated how the elements were distributed between two sub-fractions of PM_{10} (i.e., *coarse* (airborne fraction between 10 and 2.5 μm, $PM_{10\text{-}2.5}$) and *fine* (airborne fraction below 2.5 μm, $PM_{2.5}$) fraction). This approach was followed to study the element distribution in urban particulate matter for a better knowledge of both the inorganic content, especially, the elements never determined as well as the contribution of anthropogenic sources [3–7]. Briefly, few elements such as Fe and Sb showed an even distribution between the two fractions whereas some of them (i.e., Au, Ba, Ce, Cr, Cs, Hf, La, Mo, Nd, Sb, Sc, Sm, Th and Yb) showed levels more elevated in the coarse fraction than in the fine fraction; on the other hand, As, Br Ni, Rb, Se, W, and Zn displayed an opposite behavior. Finally, Co, Hg, and Zn (three anthropogenic elements) exhibited no predominant distribution between the two granulometric masses. Furthermore, in other previous papers [8,9], the authors only demonstrated the importance of PM_1 determination in areas with high anthropogenic sources (e.g., industrial emissions, combustion processes): this fraction represents almost 60% of the total mass of PM_{10} and more than 80% of the $PM_{2.5}$ in terms of granulometric fraction.

One of the most controversial topics in the environmental field with regard to the issue related to municipal solid waste (MSW) incineration is plants that produce energy by waste (waste-to-energy) [10]. The debate over incinerators typically involves business interests (representing both waste generators and incinerator firms) [11], government regulators [12,13], environmental activists [14], and local citizens [15], who must weigh the economic appeal of local industrial activity with their concerns over health and environmental risk [16–20]. The incineration is a key process in the treatment of hazardous wastes [21–23]: it has a number of outputs such as the ash and the emissions to the atmosphere of flue gas [24,25]. Before the cleaning system (e.g., filters, scrubbers, baghouse filters), the flue gases may contain particulate matter, heavy metals, dioxins, furans, sulfur dioxide, and hydrochloric acid. If plants have adequate flue gas cleaning, the pollution components to stack emissions may be significantly reduced [26,27]. For instance, fine particles can be efficiently removed from the flue gases with baghouse filters. A Danish study showed that, even if about 40% of wastes were incinerated in plants with no baghouse filters, incinerators were only responsible for approximately 0.3% of the total domestic emissions of $PM_{2.5}$ to the atmosphere in 2006 [28,29].

This paper would like to verify the considerations about the cleaning systems related to the inorganic fraction. Starting from the emission sources, sampling campaigns were performed outside the plant to understand the inorganic fraction behavior. Actually, the main question regards if the element accumulation in granulometric fractions is similar or whether there are behavior dissimilarities. Among the different analytical techniques available for the analysis, the instrumental neutron activation analysis (INAA), a nuclear analytical method, is still the main informative approach for investigating the sample without any chemical-physical treatment [30–32].

2. Materials and Methods

The sampling, performed in an area around a large incinerator in Central Italy, was 24-h long for each filter by means of a dual channel sampler, mod. Swam Dual Channel sampler (FAI Instruments, Fonte Nuova, Italy) (flux 16.7 L min^{-1}, i.e., 1 m^3 h^{-1}), equipped with $PM_{10}/PM_{2.5}/PM_1$ sampling heads, alternatively: 45 samples (15 filters PM_{10}, 18 $PM_{2.5}$, and 12 PM_1) were collected during the seasonal sampling campaign between the middle of May and the middle of October to also understand the element content and distribution. The sampling points were fixed and located in a radius of 20 m from the plant boarders, no residences were present in the area, few commercial activities were positioned over 50 m from the site. During all samplings, the incinerator operated. All the treatments of sample

storage and handling were carried out at the National Institute for Insurance against Accidents at Work's (INAIL) laboratory according to European Union (EU) regulations [33].

Samples (i.e., filter samples), blank and standards were put in nuclear-grade polyethylene cylinders (Kartell, Milan, Italy). The irradiation was performed in the rotatory rack "Lazy Susan" of the TRIGA nuclear reactor at R.C.-Casaccia ENEA: the irradiation time was 25 h at 1 MW. The rotatory rack was held at constant rotation for having a uniform thermal flux, 2×10^{12} n × cm^{-2} × s^{-1} (and relative fluency 2.34×10^{17} n × cm^{-2}): the flux stability (>99.8%) was tested irradiating the Au standard as a monitor.

For INAA analysis, primary and secondary standards were used. This procedure was followed to obtain good quality assurance and quality control (QA/QC): standard reference materials (SRMs) with high reproducibility and precision were used. These SRMs have been certified by several international proficiency tests, to which our laboratory routinely takes part. Primary standards (Carlo Erba, Milano, Italy) were Ag, As, Au, Ba, Ca, Cd, Co, Cr, Cs, Eu, Fe, Hg, Ir, K, Mo, Na, Ni, Rb, rare earth elements (REE, i.e., La, Sm, Yb, Nd, Gd, Dy, Er, Yb), Sb, Se, Sn, Sr, Tb, Th, U, W, and Zn whereas, as secondary standards, two SRMs such as GXR-3 from the U.S. Geochemical Survey (USGS), and coal fly ash (CFA 1633b) from the National Institute of Standards and Technology (NIST). It would be better to use a reference material with a matrix as similar as possible to the samples investigated: two SRMs (i.e., USGS-GXR-3 2709 and NIST 1633b), coal fly ash, along with 35 primary standards (at different concentrations, alone or in mixing standard solutions) were used for overcoming this issue.

After irradiation, γ-ray spectrometry measurements of different durations were carried out using a Ge(HP) Canberra detector (Meriden, CT, USA) (full width at half maximum 1.75 keV at 1332 keV, relative efficiency 35%; peak/Compton ratio 60.2:1) connected to a multichannel analyzer equipped with software packages (Canberra Genie 2k) for a γ-spectra analysis. For the energy and efficiency calibrations, two sources were used (i.e., a multi-peak source, BML 1517B (^{241}Am, ^{109}Cd, ^{57}Co, ^{51}Cr, ^{137}Cs, ^{88}Yr, ^{60}Co: 1 cc of this source was placed in the Kartell nuclear grade tube) and a ^{152}Eu source). The BML 1517B source was produced and certified by the ENEA National Institute of Ionizing Radiation Metrology (INMRI-ENEA) whereas the ^{152}Eu source was by the Centre Nationale pour l'Energie Atomique (CNEA), respectively.

According to the half-life time of each radionuclide [34], two gamma measurements were performed. The first series occurred after 66–70 h from the end of irradiation and the measurement time ranged between 3600 s (1 h) and 18,000 s (5 h), each irradiated sample was placed at 4 cm from the detector; the second series after three weeks from the end of irradiation and the measurement time was 24–48 h long; each sample was placed in contact with the detector.

Table 1 reports all the nuclear data and limits of detection (LODs) for the elements studied in this work.

Table 1. Nuclear data and limit of detection (LOD) of each element determined by instrumental neutron activation analysis (INAA).

Element	Product Nuclide	Half Life	γ-ray Used (keV)	LOD (μg g^{-1})	Radionuclide Interfering (keV)
Ag	$^{110\,m}$Ag	250.4 d	657.7	0.4	
As	^{76}As	26.3 h	559.2	0.008	^{122}Sb (564.0 keV)
Au	^{198}Au	2.70 d	411.8	0.001	^{152}Eu (411.0 keV)
Ba	^{131}Ba	11.5 d	496.3	10	
Br	^{82}Br	1.47 d	776.5	0.02	^{152}Eu (778.6 keV)
Cd	^{115}Cd	2.2 d	527.7	2	
Ce	^{141}Ce	32.38 d	145.4	58 [b]	
Co	^{60}Co	5.272 y	1332.5	0.86 [b]	
Cr	^{51}Cr	27.7 d	320.0	88 [b]	
Cs	^{134}Cs	2.062 y	795.7	1.2 [b]	
Dy	^{165}Dy	2.35 h	361.7	0.01 [b]	
Eu	^{152}Eu	12.7 y	1408.0	0.3 [b]	
Fe	^{59}Fe	45.1 d	1099.2	6.3	

Table 1. *Cont.*

Element	Product Nuclide	Half Life	γ-ray Used (keV)	LOD (μg g^{-1})	Radionuclide Interfering (keV)
Ga	^{72}Ga	14.3 h	630.1	0.01	^{54}Mn (834.8 keV)
Hf	^{181}Hf	42.4 d	482.2	0.25	
Hg	^{203}Hg	46.9 d	279.0	5.2 [b]	^{75}Se (279.6 keV)
Ir	^{192}Ir	74.3 d	316.5	0.001	
K	^{42}K	12.52 h	1524.7	260	
La	^{140}La	40.27 h	1596.2	3.5 [b]	
Mn	^{56}Mn	2.6 h	1810.7	0.1	
Mo	^{99}Mo	2.75 d	141.0	1	
Na	^{24}Na	15.0 h	1368.4	2.0 [b]	
Nd	^{147}Nd	11.1 d	531.0	1	
Ni	^{58}Co	70.78 d	810.7	80	
Rb	^{86}Rb	18.66 d	1076.7	0.4	
Sb	^{124}Sb	60.3 d	1690.7	6 [b]	
Sc	^{46}Sc	83.85 d	889.2	0.9 [b]	
Se	^{75}Se	120.4 d	264.6	9 [b]	^{182}Ta (264.1 keV)
Sm	^{153}Sm	1.948 d	103.1	0.41 [b]	
Sn	^{113}Sn	115.1 d	391.1	40	
Sr	^{85}Sr	64.0 d	514.0	50	e^++e^- (511.0 keV)
Ta	^{182}Ta	115.1 d	1221.2	0.2	
Tb	^{160}Tb	72.1 d	879.4	0.3 [b]	
Th	^{233}Pa	27.4 d	311.8	0.1	
U	^{239}Np	2.35 d	277.6	0.03	^{203}Hg (279.0 keV) ^{76}Se (279.6 keV)
W	^{187}W	24.0 h	685.7	0.01	
Yb	^{175}Yb	4.21 d	396.1	0.01	
Zn	^{65}Zn	243.8 d	1115.5	12 [b]	^{46}Sc (1120.1 keV)
Zr	^{95}Zr	65.5 d	724.2	80	

m: minutes; h: hours; d: days; y: years; b: values expressed as ng g^{-1}; e^++e^-: annihilation.

3. Results

3.1. Instrumental Neutron Activation Analysis (INAA) Validation

All of the analytical procedures are performed to obtain as much information as possible. For this aim, the use of a nuclear analytical technique such as INAA is strongly recommended because it allows for high sensitivity and quantification of elements to be achieved at very low (ultra-trace) concentrations. On the other hand, using nuclear analytical techniques, the problem could regard the reference material used for the analysis. This is considered a critical point: SRMs should show a composition quite similar to the investigated matrices. According to the experience of this laboratory, largely involved in round-robin comparisons with other international laboratories for both verifying the instrumental drift and quality control, the authors solved this problem by analyzing secondary reference materials [35–37] along with primary certified standards. In particular, over the mixture of primary standard solutions (obtained starting from 1 mg mL^{-1} of each one) above reported, USGS GRX-3 and NIST 1633b (coal fly ash) were used for the evaluation of the methodology. Furthermore, in the analysis of such matrices, high attention should be focused on the precision and accuracy, along with information about the area characterization on the anthropogenic sources present in the territory. Table 2 shows the comparison between our data and the relative certified values for the investigated SRMs.

Table 2. Analytical comparison (mean ± s.d.; μg g^{-1}) of standards USGS GRX-3 and NIST 1633b (coal fly ash).

Element	Product Nuclide	USGS GXR-3			NIST 1633b		
		Found	**Certified**	**Δ/*z***	**Found**	**Certified**	**Δ/*z***
As	^{76}As	4162 ± 389 (9.3)	4000 ± 450	4.1/0.24	53.1 ± 6.4 (12.1)	136.2 ± 2.6	−61.0/1.00
Ba	^{131}Ba	7934 ± 181 (2.3)	4700 ± 800	68.8/0.00	866 ± 108 (12.5)	709 ± 27	22.1/0.00
Br	^{82}Br		-	-/-	3.1 ± 0.7 (22.6)	(2.9)	6.9/0.21
Ca	^{47}Ca	99,740 ± 6600 (6.6)	141,000 ± 6000	−29.3/1.00	14,058 ± 1262 (9.0)	15,100 ± 600	−6.9/0.95
Ce	^{141}Ce	18.8 ± 2.1 (11.2)	16 ± 4	17.5/0.00	157 ± 11 (7.0)	(190)	−17.3/1.00
Co	^{60}Co	47 ± 3 (6.4)	48 ± 5	−1.9/0.74	52.2 ± 1.3 (2.5)	(50)	4.4/0.00
Cr	^{51}Cr	19 ± 1 (5.3)	19 ± 1	1.1/0.42	194.2 ± 8.8 (4.5)	198.2 ± 4.7	−2.0/0.78
Cs	^{134}Cs	192 ± 12 (6.3)	200 ± 50	−4.0/0.99	11 ± 2 (18.2)	(11)	3.3/0.37
Eu	^{152}Eu	0.48 ± 0.15 (31.2)	0.40 ± 0.10	20.0/0.06	4.1 ± 0.2 (4.9)	(4.1)	0.5/0.41
Fe	^{59}Fe	200,604 ± 52,272 (26.1)	186,000 ± 18,000	7.9/0.20	44,294 ± 339 (0.8)	77,800 ± 2300	−43.1/1.00
Hf	^{181}Hf	2.5 (-)	2.4 ± 0.2	3.8/-	6.6 ± 0.1 (1.5)	(6.8)	−2.9/0.98
La	^{140}La	9.4 ± 1.6 (17.0)	8.5 ± 1.0	10.5/0.21	87.4 ± 12.7 (14.5)	(94.0)	−7.0/0.89
Na	^{24}Na	2970 (-)	7800 ± 400	−61.9/-		2010 ± 30	-/-
Nd	^{147}Nd			-/-	75 ± 5 (6.7)	(85)	−11.4/1.00
Ni	^{58}Co	39 (-)	55 ± 5	−29.6/-	97.5 ± 59.1 (XX)	120.6 ± 1.8	−19.2/0.78
Rb	^{86}Rb	100 (-)	116 ± 10	−13.8/-	154 ± 7 (4.5)	(140)	10.0/0.00
Sb	^{124}Sb	35 ± 8 (22.9)	40 ± 3	−12.5/0.86	6 ± 1 (16.7)	(6)	−1.7/0.90
Sc	^{46}Sc	17 ± 2 (11.8)	18 ± 1	−3.9/0.21	42.6 ± 0.2 (0.5)	(41)	3.9/0.00
Se	^{75}Se		0.22 ± 0.02	-/-	12.54 ± 3.12 (24.9)	10.26 ± 0.17	22.2/0.05
Sm	^{153}Sm	3.2 (-)	1.0 ± 0.3	221.0/-	19 ± 1 (5.3)	(20)	−3.5/0.73
Sr	^{85}Sr	1140 ± 95 (8.3)	1140 ± 100	0.0/-		1041 ± 14	
Ta	^{182}Ta	0.33 (-)	0.32 ± 0.11	3.1/-	1.7 ± 0.1 (5.9)	(1.8)	−5.6/1.00
Tb	^{160}Tb	-	-	-/-	2.1 ± 0.4 (19.0)	(2.6)	−19.2/0.99
\Th	^{233}Pa	2.97 ± 0.2 (6.7)	2.90 ± 0.4	2.4/0.05	22.6 ± 2.2 (9.7)	25.7 ± 1.3	−12.1/0.99
U	^{239}Np	2.9 ± 0.4 (13.8)	3.1 ± 0.1	−8.1/0.84	8.51 ± 1.90 (22.3)	8.79 ± 0.36	−3.2/0.60
W	^{187}W	10,800 (-)	10,800 ± 600	0.0/-	-	-	
Yb	^{175}Yb		0.76 ± 0.31	-/-	7.4 ± 0.3 (4.1)	(7.6)	−2.6/0.94
Zn	^{65}Zn	219 ± 8 (3.7)	220 ± 70	−0.50/0.81	295 ± 13 (4.4)	(210)	40.5/0.00

In brackets are reported the coefficients of variation, CV (%), calculated as ratio between standard deviation and mean value × 100; Δ: difference (%) between our and USGS mean values calculated as $= \frac{(\text{our value} - \text{USGS value})}{\text{USGS value}} \times 100$; *z*: *z*-score.

As reported in previous papers [38,39], the authors refer to the precision, calculated as the coefficient of variation (CV%), for defining a mean value as good, acceptable, or unsatisfactory (i.e., <20%, between 20–30% and >30%, respectively, for concentration levels <500 μg g^{-1}; <10%, between 10–20% and >20%, respectively, for concentration levels >500 μg g^{-1}). Furthermore, the table shows the accuracy, calculated as the difference between found and certified values and reported as Δ, and the *z*-scores, which represent the distance between the raw score and the population mean in units of the standard deviation and also includes the relative uncertainties of each certified value and the measurement performed (a positive *z*-score means a value above the mean, a negative *z*-score is a value below the mean). All overall means fit into the confidence intervals. In particular, the comparison was good/acceptable for most of the elements and all the data were good in terms of precision and accuracy. Only a few elements (i.e., Ba, Na, Sm for USGS GRX-3, and As, Fe, Zn for NIST 1633b) showed poor accuracy, even if the precision was high.

3.2. PM_{10}, $PM_{2.5}$, and PM_1 Analysis

Table 3 shows the analytical data of each element investigated in this study. First, the concentrations of the three PM fractions should be noted: the mean levels of PM_{10} and $PM_{2.5}$ were below the law limit values (PM_{10} daily average 50 μg m^{-3}, PM_{10} annual average 40 μg m^{-3}, and $PM_{2.5}$ annual average 25 μg m^{-3}) [40] whereas no limits were reported for PM_1. For this last fraction, very few data are present in the literature: Roemer and van Wijnen [41] reported PM_1 levels ranging between from 20 μg m^{-3} to 26 μg m^{-3} for the background, street, and motorway sites in the Netherlands; Perez et al. [42] confirmed the scarce presence of PM_1 data on levels and speciation and reported a mean level of 19 μg m^{-3} in Barcelona from October 2005 to October 2006; Vecchi et al. [43] showed levels of 29–34 μg m^{-3} in Milan; Pakkanen et al. [44] measured 11–12 μg m^{-3} in Helsinki; and the same levels were also found by Spindler et al. [45] in rural areas in Germany. The situation was quite different as determined by Bathmanabhan and Madanayak [46]: they found hourly average PM_1 concentrations ranging between 32 and 66 μg m^{-3} near an urban roadway in Chennai city (India), where the levels depend on the meteo-climatic conditions (post-monsoon period, winter and summer seasons). Therefore, the concentrations found in this paper could be considered as quite good, considering the environmental conditions present in the area.

First, among the 36 elements investigated, their distribution in the three different fractions was not regularly distributed: for instance, Au, Ca, Cd, Co, Eu, Fe, La, Mo, Na, Ni, Sm, Sn, Ta, and Tb showed decreasing levels passing from PM_{10} to PM_1, whereas Ce, Hg, Sc, and Zn did not show any significant difference in any of the three fractions. Other elements were instead distributed between PM_{10}, $PM_{2.5}$, and PM_1 in different ways (e.g., As was at 1.0 μg m^{-3}, 0.38 μg m^{-3}, and 1.1 μg m^{-3} in PM_{10}, $PM_{2.5}$ and PM_1, respectively).

With the exception of Cd and U (their levels were below the respective LODs), our attention only focused on some elements: As, Au, Br, Ce, Co, Cr, Cs, Fe, Hg, Ni, Sb, Sc, Se, Th, and Zn. Their importance is due to different reasons such as the toxicological point of view, the identification of the anthropogenic or natural sources, or the possible common origin between them. In this way, an important example is described by bromine: its level in the atmosphere is essentially due to natural, (i.e., marine aerosol) and anthropogenic (i.e., auto-vehicular traffic, sources) [1,47]: the levels of this element were 0.22 ng m^{-3}, 0.17 ng m^{-3}, and 0.52 ng m^{-3}, respectively in PM_{10}, $PM_{2.5}$ and PM_1 with a coefficient of variation (CV%) varying between 43.5%, 55.8%, and 7.5%, respectively. It should be noted that the CV% for each element shows its concentration level variability across the whole sampling period. As can be seen, the minimum CV% is related to the PM_1 fraction, meaning a low data dispersion for this size.

The Br level in PM_{10} (0.22 ng m^{-3}) was really below the level found in downtown Rome (22.2 ng m^{-3}) [2] and the level in $PM_{2.5}$ (0.17 ng m^{-3}) was really below that found in the same city (17.1 ng m^{-3}) [1], whereas the correlation (*r*) with another important element, Sb, was very good for PM_{10} (0.9998), good for PM_1 (0.761), and less good for $PM_{2.5}$ (0.156). This occurrence (i.e., the high correlation between Br and Sn within PM_{10} and low within $PM_{2.5}$) suggests a different contribution to Br levels.

Table 3. Element mean concentration (ng m^{-3}; LOD limit of detection) in the PM_{10}, $PM_{2.5}$, and PM_1 samples investigated in this study, along with min/max values and coefficient of variation (CV%).

Element	PM_{10}		$PM_{2.5}$		PM_1	
	Mean ± st.dev. 38,500 ± 12,500	**Min–Max; CV% 18,900–62,500; 42.1;**	**Mean ± st.dev. 19,500 ± 7100**	**Min–Max; CV% 8300–37,500; 29.7;**	**Mean ± st.dev. 11,400 ± 2.600**	**Min–Max; CV% 7500–19,400; 23.7**
Ag	0.36	<LOD–0.36; -	0.44 ± 0.17	0.21–0.66; 39.6	0.16	<LOD–0.16; -
As	1.0 ± 0.4	0.48–1.3; 45.0	0.38 ± 0.21	0.10–0.70; 54.7	1.1 ± 0.2	1.0–2.0; 15.2
Au	0.349 ± 0.574	0.006–1.000; 164.4	0.006 ± 0.003	0.003–0.011; 48.0	0.003 ± 0.001	0.002–0.004; 53.9
Ba	26 ± 14	11–63; 53.0	27 ± 13	15–52; 48.9	5.9	<LOD–5.9; -
Br	0.22 ± 0.09	0.08–0.41; 43.4	0.17 ± 0.10	0.09–0.30; 55.8	0.52 ± 0.04	0.49–0.55; 7.5
Ca	681 ± 310	463–894; 45.5	0.31 ± 0.14	104–79; 47.6	<LOD	
Cd	1.6	<LOD–1.6; -	<LOD		<LOD	
Ce	0.29 ± 0.05	0.25–0.34; 16.1	0.28 ± 0.10	0.10–0.40; 35.1	0.20 ± 0.03	0.18–0.22; 12.5
Co	0.57 ± 0.53	26–118; 92.9	0.29 ± 0.07	0.20–0.40; 24.4	0.14 ± 0.01	0.12–0.15; 8.2
Cr	3.6 ± 0.8	2.9–4.5; 21.9	3.4 ± 1.0	2.0–5.4; 30.1	5.9 ± 1.6	4.3–7.6; 27.6
Cs	0.058 ± 0.010	0.039–0.070; 16.8	0.041 ± 0.015	0.026–0.066; 35.3	0.054 ± 0.010	0.047–0.061; 18.0
Eu	0.014 ± 0.001	0.0081–0.015; 12.5	0.010 ± 0.004	0.0057–0.017; 38.2	0.008 ± 0.000	7.7–7.8; 3.0
Fe	461 ± 154	283–560; 33.5	292 ± 131	126–518; 44.8	156 ± 137	130–333; 88.1
Ga	<LOD		<LOD		<LOD	
Hf	0.036 ± 0.008	0.031–0.057; 21.7	0.019 ± 0.001	0.011–0.030; 35.4	0.025 ± 0.012	0.017–0.034; 48.1
Hg	0.12 ± 0.02	0.10–0.15; 18.1	0.10 ± 0.03	0.08–0.20;29.8	0.12 ± 0.06	0.07–0.16; 45.6
K	94	<LOD–94; -	73 ± 53	10–155; 71.8	160 ± 28	141–180; 17.2
La	0.34 ± 0.03	0.30–0.36; 9.0	0.25 ± 0.08	0.10–0.30; 31.7	0.14 ± 0.03	0.12–0.16; 22.4
Mo	1.2 ± 0.3	0.97–1.5; 21.7	0.68 ± 0.08	0.66–0.69; 1.1	<LOD	
Na	128 ± 53	78–301; 41.2	92 ± 84	11–252; 90.9	26 ± 3	24–28; 12.2
Nd	<LOD		<LOD		<LOD	
Ni	3.8 ± 1.6	2.8–5.7; 42.6	2.7 ± 0.5	2.0–3.3; 18.5	0.18	<LOD–018; -
Rb	0.63 ± 0.21	0.39–0.76; 33.2	0.61 ± 0.32	0.20–1.2; 51.4	1.0 ± 0.1	0.92–1.1; 8.5
Sb	2.5 ± 0.3	1.9–3.0; 1.7	3.1 ± 2.1	0.9–8.1; 68.7	2.9 ± 1.4	1.5–4.3; 48.0
Sc	0.036 ± 0.012	0.028–0.050; 33.2	0.039 ± 0.022	0.013–0.093; 58.1	0.040 ± 0.046	0.011–0.094; 114.7
Se	0.75 ± 0.06	0.69–0.98; 8.4	0.79 ± 0.44	0.30–1.5; 55.0	1.0 ± 0.1	0.10–1.1; 6.1
Sm	0.051 ± 0.003	0.045–0.054; 7.2	0.035 ± 0.012	0.014–0.049; 34.7	0.022 ± 0.001	0.022–0.023; 3.2
Sn	2.1	<LOD–2.1; -	1.8 ± 0.5	1.5–2.2; 28.0	<LOD	
Sr	<LOD		<LOD		<LOD	
Ta	0.016 ± 0.009	0.022–0.112; 54.5	0.013 ± 0.011	0.006–0.035; 81.5	0.007	<LOD–0.007; -
Tb	0.021 ± 0.008	0.012–0.026; 38.3	0.016 ± 0.005	0.009–0.022; 33.2	0.010	<LOD–0.010; -
Th	47 ± 9	35–54; 18.7	46 ± 16	25–82; 35.5	32 ± 8	26–38; 25.7
U	<LOD		<LOD		<LOD	
W	0.23 ± 0.04	0.19–0.29; 15.0	4.8 ± 3.0	0.2–11; 62.7	0.30 ± 0.06	0.26–0.35; 20.6
Yb	0.001	<LOD–0.001; -	0.001 ± 0.000	0.001–0.002; 24.1	0.001	<LOD–0.001; -
Zn	110 ± 24	77–137; 21.7	113 ± 23	77–140; 20.6	131 ± 28	106–161; 21.4

In particular, sources of Br within particles larger than 1 µm differ from the sources of Br in submicron particles.

Regarding the protection of human health, very few elements showed limit values. In European legislation, As, Cd, and Ni should be at levels below 6.0 ng m^{-3}, 5 ng m^{-3}, and 20 ng m^{-3} (actually, these target values will be entered into force on December 2020) whereas the World Health Organization (WHO) suggests [48] a guide value for Cd of 5 ng m^{-3}: in all cases, our data were much lower than those fixed; even the maximum values were significantly below these levels.

Particular attention should be given to the CV% whose meaning has just been reported above: it ranged between 9% and 164% in PM_{10}, between 18% and 91% in $PM_{2.5}$, and between 7% and 114% in PM_1. In particular, except for a few cases in PM_{10} (Au, CV% 164%; Co, 92.9%), $PM_{2.5}$ (K, 71,8%; Na, 90.9%; Ta, 81.5), and PM_1 (Fe, 88.1%; Sc, 114.7), the CV% in these three fractions were below 60%, which means that the elements in these fractions showed slight variations and that not many sources influenced the element levels. This last information was also confirmed by the good correlation reported in Figure 1 between the various fractions (PM_{10} vs. $PM_{2.5}$: equation curve y = 0.328x + 7.252, r^2 = 0.635; $PM_{2.5}$ vs. PM_1: y = 0.521x + 2.817, r^2 = 0.551; PM_{10} vs. PM_1: y = 0.112x + 9.139, r^2 = 0.150). The last correlation (PM_{10}/PM_1) was not so good, which is not surprising considering the large difference between these two sizes.

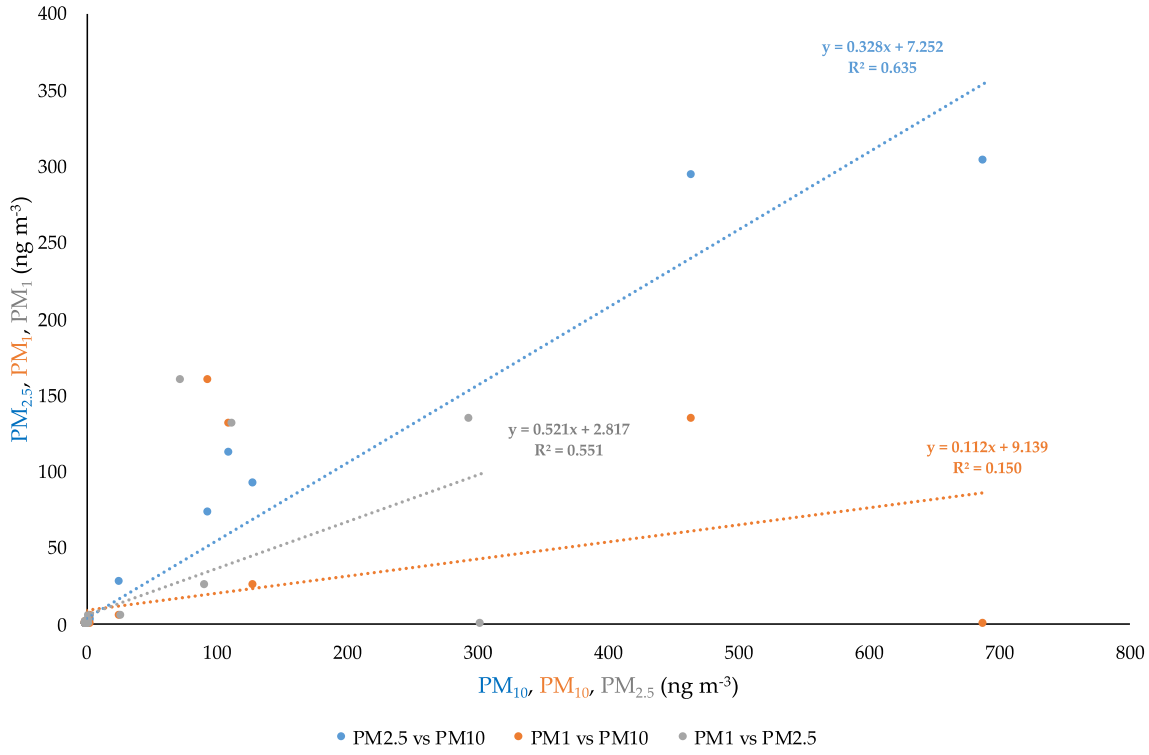

Figure 1. Relationship between the concentration elements in the PM fraction: correlation curves, linear equations, and regression coefficients (R^2).

On the other hand, the correlations between elements in each fraction (Table 4) confirmed the common sources for all elements, both natural (crustal origin) and anthropogenic (plant emissions and auto-vehicular traffic): the elements showing *r*-values above 0.6 were considered well correlated [1,2,49] such as Br, Sm, Au, Th, Ce, Ni, Eu, and Ag, ($r > 0.8$). Regarding the toxic elements, it should be underlined that the correlation between Ni and the other elements was not good, except with the rare earth elements (REEs), meaning a main component of natural sources for this element. For Cr and As, which are largely diffused in nature, the situation was slightly different: over the natural origin, their presence in the atmosphere could be due to auto-vehicular traffic and industrial emissions (e.g., metallurgical industries, coal-fired power plants, galvanic industries, waste incinerators).

Table 4. Element Pearson's correlation between the different PM-fractions ($PM_{2.5}$ vs. PM_{10}; PM_1 vs. PM_{10}; PM_1 vs. $PM_{2.5}$). In *italics* are reported the correlations > 0.6.

Na	W	As	Br	La	Sm	Au	Ca	Ba	Rb	Th	Cr	Ce	Fe	Sb	Ni	Sc	Se	Zn	Cs	Co	Eu	Ta	Ag	
1	0.003	0.079	*0.943*	*0.692*	0.529	−0.311	0.475	−0.016	0.241	*0.817*	−0.430	*0.807*	0.240	*0.974*	*0.725*	*0.841*	−0.280	0.047	0.152	*0.803*	*0.882*	*0.944*	0.166	**Na**
	1	0.248	*0.772*	*0.952*	*0.986*	0.507	*0.974*	−0.313	0.475	*0.648*	−0.566	*0.635*	*0.708*	0.474	−0.531	*0.972*	−0.278	0.575	*0.752*	*0.708*	*0.979*	*0.996*	0.406	**W**
		1	*0.793*	0.054	0.333	−0.509	0.274	−0.580	0.446	0.673	*0.651*	*0.660*	*0.629*	*0.999*	−0.559	0.542	*0.726*	−0.516	−0.299	*0.853*	0.185	*0.993*	0.375	**As**
			1	0.485	0.302	−0.537	0.242	0.001	0.475	*0.648*	−0.217	*0.635*	0.377	*0.998*	−0.531	*0.803*	0.093	−0.267	0.026	*0.941*	*0.636*	*0.996*	0.406	**Br**
				1	0.458	−0.388	0.402	−0.116	0.320	*0.767*	−0.258	*0.756*	0.402	*0.989*	*0.666*	*0.865*	−0.190	−0.094	−0.027	*0.804*	0.591	*0.968*	0.246	**La**
					1	*0.704*	*0.999*	*0.914*	*0.754*	*0.886*	*0.678*	*0.893*	*0.737*	0.242	*0.944*	*0.871*	−0.420	0.563	*0.737*	−0.220	*0.999*	0.136	*0.802*	**Sm**
						1	−0.825	0.542	*0.990*	−0.488	*0.970*	0.502	*0.987*	0.328	*0.609*	−0.460	*0.848*	*0.923*	*0.987*	−0.350	*0.851*	0.428	*0.998*	**Au**
							1	*0.873*	0.074	*0.902*	0.182	*0.895*	0.099	*0.922*	*0.831*	*0.915*	0.475	−0.324	−0.099	*0.913*	*0.678*	*0.875*	−0.003	**Ca**
								1	0.498	*0.989*	−0.248	*0.991*	*0.614*	−0.545	*0.997*	*0.900*	−0.215	−0.217	−0.222	−0.304	*0.645*	−0.452	*0.664*	**Ba**
									1	*0.980*	−0.061	*0.976*	−0.145	*0.801*	*0.941*	*0.986*	0.248	−0.086	0.145	*0.787*	*0.758*	*0.731*	−0.244	**Rb**
										1	*0.917*	*0.636*	*0.947*	0.170	*0.730*	*0.601*	*0.751*	*0.849*	*0.947*	−0.193	*0.925*	0.275	*0.975*	**Th**
											1	0.325	*0.752*	0.505	0.443	−0.242	*0.614*	−0.565	*0.910*	−0.151	0.504	*0.615*	*0.991*	**Cr**
												1	−0.476	0.546	*0.999*	*0.984*	−0.100	0.261	0.476	−0.527	*0.936*	0.453	−0.562	**Ce**
													1	*0.992*	−0.441	0.490	0.572	*0.660*	-0.333	*0.842*	0.103	*0.999*	0.497	**Fe**
														1	−0.212	0.380	*0.952*	*0.890*	*0.761*	*0.941*	0.150	*0.966*	*0.692*	**Sb**
															1	*0.990*	−0.061	0.223	0.441	0.560	*0.921*	0.488	−0.529	**Ni**
																1	*0.779*	*0.921*	−0.398	0.531	0.333	*0.943*	*0.747*	**Sc**
																	1	−0.556	−0.113	*0.836*	0.322	*0.999*	0.446	**Se**
																		1	*0.736*	−0.197	*0.876*	−0.343	*0.988*	**Zn**
																			1	*0.879*	0.377	*0.980*	0.300	**Cs**
																				1	−0.103	*0.956*	*0.718*	**Co**
																					1	*0.618*	−0.391	**Eu**
																						1	0.560	**Ta**
																							1	**Ag**

Table 4. *Cont.*

Na	W	As	Br	La	Sm	Au	Rb	Th	Cr	Ce	Fe	Sb	Sc	Se	Zn	Cs	Co	Eu	Ta	Ag	
1	0.108	0.213	*0.638*	0.559	0.512	*0.987*	*0.973*	0.139	*0.982*	−0.155	−0.214	*0.648*	0.257	0.230	−0.016	*0.900*	0.356	−0.455	*0.726*	*0.953*	**Na**
	1	*0.813*	0.061	*0.999*	*0.920*	*0.920*	*0.922*	*0.696*	*0.874*	*0.708*	−0.447	0.074	*0.674*	*0.901*	*0.976*	*0.912*	−0.097	*0.958*	0.181	*0.949*	**W**
		1	*0.967*	0.356	−0.085	*0.710*	*0.657*	−0.464	*0.735*	0.450	*0.989*	*0.970*	−0.492	−0.130	0.099	*0.675*	*0.976*	−0.026	*0.991*	*0.602*	**As**
			1	*0.948*	*0.985*	*0.764*	*0.809*	*0.842*	*0.742*	*0.850*	*0.751*	0.156	*0.923*	0.087	−0.487	*0.876*	−0.532	*0.949*	0.049	*0.851*	**Br**
				1	*0.915*	−0.278	0.347	*0.983*	0.278	*0.999*	0.160	*0.677*	*0.769*	*0.674*	−0.146	−0.341	*0.606*	0.459	*0.604*	0.418	**La**
					1	−0.483	*0.645*	*0.979*	0.450	*0.982*	0.132	−0.499	*0.972*	*0.989*	*0.930*	−0.524	0.479	*0.954*	−0.402	*0.608*	**Sm**
						1	*0.898*	*0.736*	*0.845*	*0.747*	0.396	−0.017	*0.714*	*0.924*	*0.987*	*0.887*	0.040	*0.972*	−0.125	*0.929*	**Au**
							1	*0.914*	*0.630*	*0.920*	−0.081	−0.304	*0.901*	*0.998*	*0.987*	*0.693*	0.282	*0.996*	−0.199	*0.762*	**Rb**
								1	*0.875*	0.225	*0.996*	*0.885*	−0.271	0.109	0.332	*0.831*	*0.896*	−0.263	*0.930*	*0.770*	**Th**
									1	0.554	*0.622*	0.269	*0.742*	−0.133	0.362	*0.984*	0.216	*0.851*	0.371	*0.992*	**Cr**
										1	0.378	0.003	*0.728*	*0.932*	*0.990*	*0.878*	0.020	*0.977*	−0.105	*0.922*	**Ce**
											1	*0.997*	*0.824*	0.228	*0.642*	−0.134	*0.992*	*0.690*	*0.999*	−0.451	**Fe**
												1	−0.453	−0.078	0.257	*0.979*	−0.135	*0.667*	*0.698*	*0.964*	**Sb**
													1	*0.997*	*0.833*	−0.013	0.110	0.270	0.337	*0.662*	**Sc**
														1	0.219	*0.883*	−0.379	0.486	*0.881*	*0.840*	**Se**
															1	*0.973*	0.139	*0.639*	*0.628*	*0.985*	**Zn**
																1	*0.754*	*0.604*	*0.628*	*0.985*	**Cs**
																	1	*0.621*	*0.976*	*0.660*	**Co**
																		1	0.402	*0.608*	**Eu**
																			1	*0.608*	**Ta**
																				1	**Ag**

Table 4. *Cont.*

Na	W	As	Br	La	Sm	Au	Rb	Th	Cr	Ce	Fe	Sb	Sc	Se	Zn	Cs	Co	Eu	Ta	Ag	
1	0.400	*0.665*	−0.345	−0.310	0.582	*0.932*	−0.062	*0.861*	*0.986*	0.284	*0.693*	*0.879*	*0.919*	−0.573	*0.809*	−0.461	*0.875*	−0.031	−0.281	*0.996*	**Na**
	1	0.063	0.096	−0.073	*0.950*	*0.966*	−0.539	*0.995*	*0.898*	*0.795*	0.197	0.428	0.498	0.140	*0.986*	−0.018	−0.461	−0.662	*0.793*	*0.751*	**W**
		1	*0.976*	*0.925*	−0.001	−0.547	*0.632*	−0.403	*0.699*	−0.328	*0.993*	*0.992*	*0.979*	*0.984*	0.468	*0.944*	*0.987*	−0.505	0.330	*0.862*	**As**
			1	0.299	*0.996*	*0.882*	*0.717*	*0.947*	*0.774*	*0.912*	0.032	−0.210	−0.287	0.090	*0.921*	0.245	0.246	*0.815*	*0.911*	*0.610*	**Br**
				1	*0.878*	0.473	*0.983*	*0.610*	0.293	*0.986*	−0.580	−0.367	−0.292	*0.627*	-0.552	*0.742*	0.332	*0.991*	*0.987*	0.032	**La**
					1	*0.655*	*0.919*	*0.769*	0.496	*0.998*	−0.387	−0.153	−0.075	−0.440	*0.722*	−0.576	0.117	*0.968*	*0.998*	0.251	**Sm**
						1	0.585	*0.988*	*0.872*	*0.828*	−0.142	−0.376	−0.448	−0.083	*0.975*	0.074	0.410	*0.703*	*0.827*	*0.712*	**Au**
							1	*0.887*	*0.669*	*0.964*	−0.183	0.060	0.139	−0.240	*0.852*	−0.389	−0.097	*0.894*	*0.963*	0.450	**Rb**
								1	*0.849*	−0.094	*0.936*	*0.993*	*0.999*	*0.914*	*0.664*	*0.839*	*0.997*	−0.286	0.097	*0.958*	**Th**
									1	*0.660*	0.248	*0.608*	*0.660*	0.058	*0.999*	−0.053	−0.503	−0.061	*0.658*	*0.867*	**Cr**
										1	−0.122	−0.358	−0.430	−0.064	*0.970*	0.094	0.392	*0.717*	*0.838*	*0.698*	**Ce**
											1	*0.956*	−0.447	*0.884*	−0.313	*0.874*	*0.647*	−0.102	0.487	*0.762*	**Fe**
												1	*0.884*	0.413	*0.919*	0.310	*0.779*	0.116	0.319	*0.992*	**Sb**
													1	0.110	0.039	0.218	−0.058	*0.944*	*0.992*	−0.319	**Sc**
														1	*0.768*	0.571	*0.919*	0.311	0.021	*0.985*	**Se**
															1	−0.276	*0.763*	−0.008	−0.407	*0.975*	**Zn**
																1	−0.455	−0.475	0.407	*0.975*	**Cs**
																	1	0.581	−0.252	*0.900*	**Co**
																		1	*0.998*	−0.251	**Eu**
																			1	0.251	**Ta**
																				1	**Ag**

Studies performed in European Union (EU) countries have shown chromium values in ambient air ranging between 4 and 70 ng m^{-3} in urban areas, and between 5 and 200 ng m^{-3} in industrial areas. Arsenic values in ambient air, on the other hand, vary between 1 and 3 ng m^{-3} in urban areas and between 20 and 30 ng m^{-3} in industrial areas [48,50,51].

In this study, these two elements (i.e., Cr and As) defined as carcinogenic compounds for human health (Group 1) by the International Agency for Research on Cancer (IARC) and the Environmental Protection Agency (EPA) [48,50], showed good correlations in all cases, meaning that they have common origins. This consideration was strengthened by their correlations with Fe, an element widely present in the crustal composition.

The correlation is really important when analyzing the correlation data for the REEs: their good values (most of them showed a $r > 0.8$) allow to take information about the evaluation of data quality, to understand the mass transport events because their presence affects the sample homogeneity, and the particulate matter composition and aging [52,53].

3.3. Comparison with Other Scenarios Worldwide

Table 5 shows a comparison among the element levels in the three fractions determined in this study and similar determinations in other locations. First, it should be underlined that in the literature, very few papers have dealt with such evaluations in different fractions: basically, the main fractions considered are PM_{10} and $PM_{2.5}$, whereas few authors have approached the PM_1 fraction. In the table, different scenarios are reported: PM_{10} and $PM_{2.5}$ were determined around a waste-to-energy plant in the Central of Italy; PM_{10} around a hazard waste landfill (HWL) in Spain; $PM_{2.5}$ sampled in different areas around Shanghai; and PM_{10}, $PM_{2.5}$, and PM_1 in downtown Algiers and Rome [1,2,26,54–56]. Preliminarily, the levels determined in this study were lower than those reported by Buonanno et al. [26], where PM_{10} and $PM_{2.5}$ were determined around a waste plant: in fact, the difference was not that great, but As, Hg, and Sb showed lower levels whereas Cd and Ni had similar values. No information on fraction PM_1 has been reported for that site. On the other hand, the comparison between similar fractions (PM_{10}) investigated at this site and around the HWL plant in Spain [54] reported almost 10-times lower levels at the Spanish site (e.g., Cr 3.6 vs. 0.4 ng m^{-3}; Ni 3.8 vs. 0.58 ng m^{-3}; Hg 0.12 ng m^{-3} vs. not detected). Furthermore, the comparisons with the data determined in downtown Rome [1,2] or in urban, residential, suburban, or industrial locations around Shanghai [55] showed significant differences between the three sites. Finally, in Algiers [56], where the three fractions were determined, the levels were very high (e.g., As at 59.8–178.5 ng m^{-3} for PM_{10}, 48.5–137.9 ng m^{-3} for $PM_{2.5}$, 38.4–70.9 ng m^{-3} for PM_1; Cr 57.3–100.2 ng m^{-3}, 30.7–60.2 ng m^{-3}, 7.3–32.3 ng m^{-3}, respectively). Among the different reasons for these very high levels found in Algiers, the authors reported "poor combustion of the car fleet, which is increasingly dieselized, aging and poorly maintained and where the use of unleaded gasoline is still very low", a scenario quite different with respect to that present in European countries. Some comments could be also withdrawn in relationship to the PM_x amount: in this case, the global situation is quite different. First, no comparison was possible with the data collected around the waste-to-energy plant in Cassino, Italy [26] (data not available in the paper). Regarding the comparison with the data from Rome (site B in Table 5), some elements determined in this study showed a higher presence in relation to their respective PM_{10} and $PM_{2.5}$ levels: among all elements, Ba, Cd, Co, Fe, La, Ni, Se, and Zn in PM_{10} and Ba, Co, Cr, Fe, La, Mo, Ni, Se, and Zn in $PM_{2.5}$ should be considered for their environmental and human health roles. Similarly, the same comparison with the data collected at sites D and E (Table 5) described a different situation. Each site showed minimum and maximum data for each element, so the comparison occurred with low and high values. Looking at the PM data, both sites evidenced data lower than those determined in this study, especially in Algiers. At this site, only Ca in the PM_{10} and $PM_{2.5}$ fractions and Cr in PM_1 was displayed in proportion to the PM measures.

Table 5. Element concentrations (ng m^{-3}) in PM_{10}, $PM_{2.5}$, and PM_1 in comparison with other sites worldwide.

Element	This Study			A		B		C	D	E		
	PM_{10} 38,500	**$PM_{2.5}$ 19,500**	**PM_1 11,400**	**PM_{10} N/A**	**$PM_{2.5}$ N/A**	**PM_{10} 58,200**	**$PM_{2.5}$ 29,300**	**PM_{10} N/A**	**$PM_{2.5}$ 62,500**	**PM_{10} 137,000**	**$PM_{2.5}$ 47,030**	**PM_1 26,005**
Ag	0.36	0.44	0.16			0.176			0.01–1.20			
As	1.0	0.38	1.1	4.16	2.67	1.35	1.06	0.04–0.42	4–73	59.8–178.5	48.5–137.9	38.4–70.9
Au	0.349	0.006	0.0028	1.014	0.541	0.008	0.009					
Ba	26	27	5.9	42.1	12.5	12.8	3.76		1–34	4442–5986	3746–4811	2969–4120
Br	0.22	0.17	0.52	66	44.5	22.2	17.1					
Ca	680	310	<LOD	3390	1870	1500				20–160	4220–7280	2830–4250
Cd	1.6	<LOD	<LOD	1.25	0.824	0.526		0.05–0.08	0.2–12.2			
Ce	0.29	0.28	0.20	0.752	0.180	0.843	0.130		0.2–4.1			
Co	0.57	0.29	0.14	0.379	0.192	0.379	0.167		0.1–4.4			
Cr	3.6	3.4	5.9	8.21	2.09	7.28	3.03	0.40–5.64	1–134	57.3–100.2	30.7–60.2	7.3–32.3
Cs	0.058	0.041	0.054	0.151	0.042	0.151	0.047					
Eu	0.014	0.010	0.0077	0.039	0.0096	0.012	0.0011					
Fe	461	292	156	643	121	566	74		192–4150	11,400–17,000	6140–8270	2620–3970
Hf	0.036	0.019	0.025	0.117	0.053	0.020	0.018					
Hg	0.12	0.10	0.12	1.65	0.722	1.07	0.818	n.d.				
K	94	73	160	4030	1980	1100						
La	0.34	0.25	0.14	3.79	0.845	0.188	0.022		0.02–2.65			
Mo	1.2	0.68	<LOD	4.56	1.54	2.10	0.748			11.2–123.3	8.9–89.3	7.2–50.5
Na	128	92	26	3660	2120	420						
Nd	<LOD	<LOD	<LOD	-	-	0.245	<LOD					
Ni	3.8	2.7	0.18	2.87	2.87	4.54	3.54	0.58–4.76	2–56			
Rb	0.63	0.61	1.0	5.44	2.32	2.19	1.82					
Sb	2.5	3.1	2.9	10.8	4.24	9.22	3.60		12–45			
Sc	0.036	0.039	0.040	0.054	0.004	0.046	0.003			0.023–0.16	0.021–0.14	0.014–0.14
Se	0.75	0.79	1.0	1.01	0.843	0.687	0.567		0.1–9.3	26.9–57.8	16.2–44.2	8.2–31.6
Sm	0.051	0.035	0.022	0.041	0.006	0.053	0.004					
Sn	2.1	1.8	<LOD									
Sr	<LOD	<LOD	<LOD	50.8	15.7					530–1192	339–895	205–647
Ta	0.016	0.013	0.0066									
Tb	0.021	0.016	0.010									
Th	47	46	32			0.204	0.027					
U	<LOD	<LOD	<LOD						0.01–0.56			
W	0.23	4.8	0.30	1.07	0.549	1.25	0.636					
Yb	0.0009	0.0011	0.00099	0.043	0.020	0.015						
Zn	110	113	131	96.4	64.3	80.0	58.0		20–1163			

LOD: limit of detection; n.d.: not detected in the publication; N/A: not available; A: around the waste-to-energy plant in Cassino, Italy [26]; B: downtown Rome, Italy [1,2]; C: around the hazardous waste landfill of Castellolí, Spain [54]; D: urban/residential/suburban/industrial areas around Shanghai, China [55]; E: downtown Algiers, Algeria [56].

The identification of natural and anthropogenic origins of the investigated elements was an important aspect of this research: in comparison with previous studies or speculation of the sources, the authors focused their attention on the study of the Enrichment Factors (EFs). This approach allows the element presence to be correlated with respect to the same element abundance in the upper continental crust [49,57]. The EFs were calculated according to the equations reported in Misaelides et al. [58] and Bergamaschi et al. [59] using La as the normalizing element: if the EF value is below 10, the element has a crustal origin and therefore is defined as "no enriched element"; in contrast, if the EF value is higher than 40–50, the elements are of anthropogenic origin and are called "elements enriched"; values between these two thresholds show a mixed origin of the element investigated (long-transport phenomena from other natural and/or anthropogenic sources). Figure 2 shows the EF profile for all of the elements investigated in the three fractions. As can be seen, most of the considerations above reported were confirmed: Ni, Cr, Fe, Rb, Ni, Br and As can be considered as no enriched elements (their EFs were below 10), in other words, having a crustal origin. Actually, the As in the PM_1 fraction showed an EF almost at the border (i.e., EF 44.5), meaning a contribution from anthropogenic sources. A similar condition was found for Hg, whose values were in the range 10–50. On the other hand, elements such as Zn, Sb, Ag, Sc, Cd, and Au showing EFs >50 (up to 3413 for Au in the PM_{10}) came from anthropogenic sources (e.g., the waste plant, the heavy traffic): among them, Sb and Cd involve problems related to human health, but their low levels, compared with their relevant limit/guideline values, should not raise an alarm in the population.

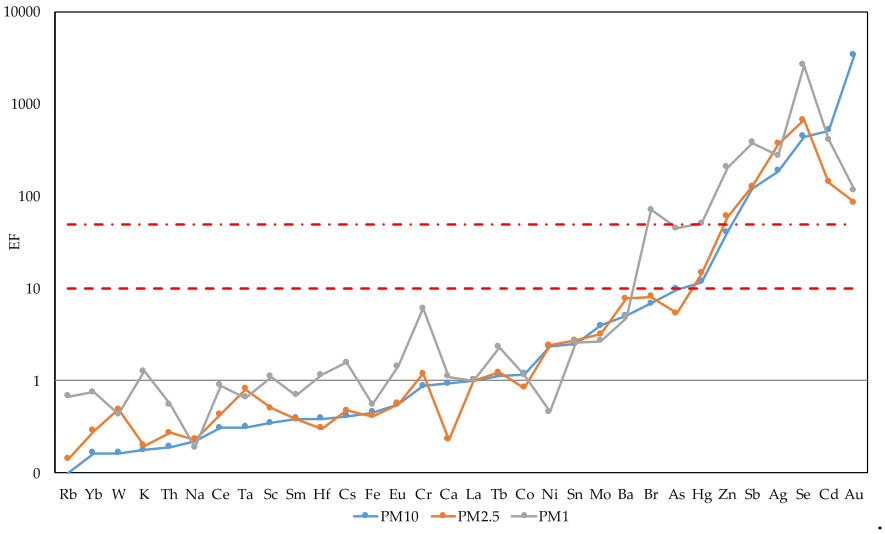

Figure 2. Enrichment Factors of all the elements investigated in this study in the three PM fractions. La was used as the normalized agent.

3.4. Statistical Analysis

For evidencing the relationship between the elements and possible similarities among the fractions, a statistical approach was performed, in particular, a source discrimination analysis followed by a chemometric methodology allowed us to gain some information on the fractions sampled.

The uncertainties due to variation in counting geometry is a typical error in the INAA methodology, depending on the equipment and sample-holder used. It can be minimized by means of the Aspinall protocol [60], in other words, the application of the source discrimination approach in relation to the Sc (considered as the internal standard due to its high accuracy in the determination), calculated according to the following formula:

$$\text{Source Discrimination} = \frac{1}{[\text{Sc}]} \times \left([\text{Cs}] + [\text{Ta}] + \frac{[\text{Rb}]}{100} + \frac{[\text{Th}] + [\text{La}] + [\text{Ce}]}{10} \right) \quad (1)$$

This procedure, also used when the sample numbers are few, allows for very close differences to be discriminated among the samples. Figure 3 shows the source discrimination equation applied to the samples investigated in this study: as can be seen, all the samples could be grouped in a single cluster. This means that the sampled aerosol, PM_{10}, $PM_{2.5}$, and PM_1, come from a single common source. Although this analysis allows us to draw such information, the elements involved (i.e., Ce, Cs, La, Rb, Sc, Ta and Th) were not enough to discriminate the samples satisfactorily.

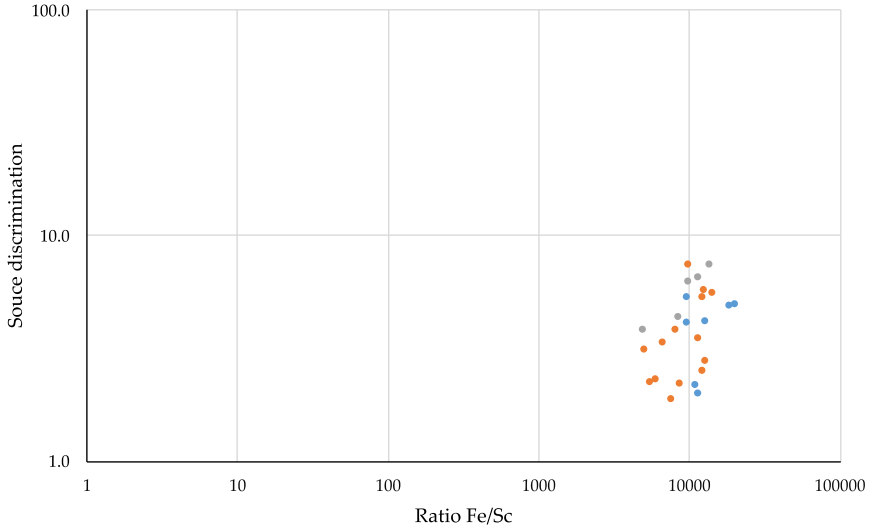

Figure 3. Multiple regression analysis: plot of the discrimination factor (source discrimination) versus Fe/Sc abundance ratio (blue: PM_{10}; orange: $PM_{2.5}$; grey: PM_1).

These data should be considered preliminary: in fact, the results are subjected to large uncertainty. To overcome these doubts, advanced statistical methods, quite similar to those used in cultural heritage studies (e.g., provenance) or in the quality control of goods, were used. Cluster analysis (CA) and multivariate analysis [61,62] manage to describe a source apportionment character through a wide "chemical composition profile" [37].

Statistical analysis was carried out with Tanagra open-source software [63] using the centroid merge method and the Euclidean distance as a measure of proximity [64,65]. First, application of the hierarchical cluster analysis (HAC) gives a dendrogram showing that the three-fraction aerosol samples can be grouped in the following three clusters:

1st Cluster (eleven members): W, Zn, Ba, Cr, Sc, Ag, Rb, Ce, Th, Sb, Ta.
2nd Cluster: (ten members): Br, Co, Eu, Sm, Mo, Se, Fe, Ni, Hf, Tb.
3rd Cluster (six members): As, Ca, Na, Cs, La, Au.

Starting from this consideration, the chemometric investigation was addressed to validate the information about the samples with a high percentage of accuracy. Particularly, considering the three different size granulometric fractions as the main characteristics and the elements determined in the samples as variables, the discriminating factorial analysis was applied. The main purpose of the discriminant function analysis is to determine whether groups (i.e., the three aerosol fractions) differ with regard to the mean of a variable, and then to use that variable to predict group membership.

The application of the principal component analysis (PCA) to the entire dataset managed to obtain three principal components describing 99% of the total variance of the data matrix (only with two components was almost 81% of the data described). Afterward, using the discriminating factorial analysis, the composition linear models of the discriminant functions were found. The statistical test showed the separation of the samples in two groups (Figure 4): the principal one was formed by the PM_{10} and $PM_{2.5}$ fractions whereas the second cluster was made of PM_1 aerosol filters. These

findings confirm the strict relationship between PM_{10} and $PM_{2.5}$ about the sources, whereas similar evidence shows possible additional sources to the PM_1 contribution. This occurrence can be explained considering previous studies on aerosol size distributions [8,66]. In fact, they have highlighted that the $PM_{2.5}$ convention includes particles from both fine and coarse modes. The aerosol size spectra showed that there is a region where the tails of the PM_{10} and $PM_{2.5}$ may overlap to some extent. In this region, PM is dominated neither by anthropogenic sources (essentially fine PM) nor by natural sources (essentially coarse PM). Thus, this means that the PM2.5 fraction "contains" PM_{10}. For this reason, it could be stated that PM_{10} and $PM_{2.5}$ have the same origin, whereas the presence of other sources (for instance, a highway close to site) is relevant for the PM_1 fraction.

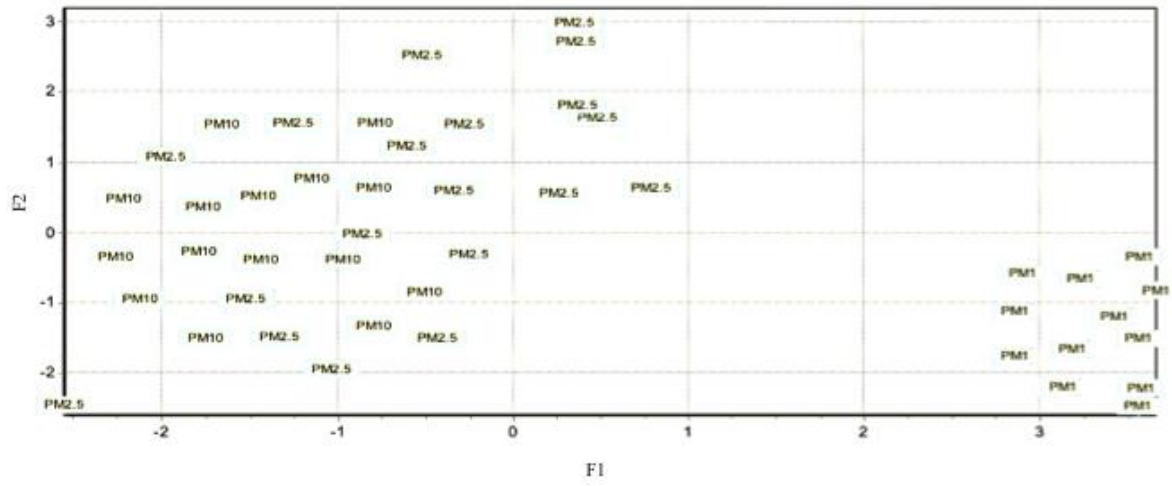

Figure 4. Airborne filter identification in two groups using the discriminant functions.

Finally, the loadings and the percentage of the variance obtained for each of the components are reported in Table 6. Variable factor loadings were used to identify pollution sources and to evaluate the anthropogenic and natural contributions at the sampling site. Only variables with factor loadings greater than 0.5 (in italics in the table) were taken into account in order to characterize the source of pollution. Factor 1 is related to elevated local non-crustal contribution, as expressed by the factor loadings in Br and Cr, whereas F3 is related to both crustal and anthropogenic contributions, by the factor loadings in Na and Zn as well as F4 by the factor loadings in Th and As.

Table 6. Results of principal component analysis (PCA) applied to the PM_{10}, $PM_{2.5}$, and PM_1 samples. In italics are presented are the factor loadings greater than 0.5.

Element	F1	F2	F3	F4
Sc	−0.825	−0.212	−0.158	0.052
Fe	−0.746	−0.408	−0.103	0.214
La	−0.725	−0.065	*0.517*	−0.032
Ba	−0.624	−0.125	−0.089	−0.399
Br	*0.566*	−0.613	0.212	−0.224
Cr	*0.544*	−0.485	−0.062	0.280
Na	−0.543	0.036	*0.616*	−0.130
Se	−0.066	−0.854	−0.163	−0.343
Sb	−0.276	−0.649	−0.557	−0.023
Cs	−0.160	−0.645	0.411	0.065
As	0.129	−0.544	0.345	*0.506*
Zn	0.348	0.027	*0.690*	−0.275
W	−0.213	0.236	−0.156	−0.755
Th	−0.372	0.329	−0.310	*0.562*
Co	−0.372	0.211	0.461	0.285
% variance	24%	19%	14%	1%

4. Conclusions

The inorganic characterization of the three different PM-fractions is an important issue in environmental science to both identify the contamination sources and in attempting a risk assessment according to the element content. This paper focused attention on the inorganic fraction of PM_{10}, $PM_{2.5}$, and PM_1 airborne filters sampled in a site close to an incineration plant: the levels of about 40 elements were determined, and the correlations between the elements and PM-fractions showed good correlation of PM_{10} vs. $PM_{2.5}$ and the worst between PM_{10} vs. PM_1. The EFs were studied for all the fractions: among the highly toxic metals, Sb and Cd showed a well-defined anthropogenic contribution whereas Hg and As only did partially. A statistical approach was performed to identify similarities among the filter samples. From the source discrimination test, similar behavior was evaluated overall for the samples; the HAC divided the elements in three main clusters whereas the PCA allowed the samples to be separated into two groups, in other words, one formed by PM_{10} and $PM_{2.5}$ filters and one only by PM_1 filters (the two groups were well-separated between them), meaning a different element contribution to this fraction coming from other relevant sources present at the site (and not identified because this was not part of the study).

Author Contributions: Conceptualization, G.C. and P.A.; Methodology, P.A.; Software, M.M. and P.C.; Validation, M.M., A.R., and A.P.; Formal analysis, M.L. and A.R.; Investigation, M.L. and P.C.; Resources, A.R. and P.C.; Data curation, M.M., A.R., and M.L.; Writing—original draft preparation, A.R. and P.A.; Writing—review and editing, P.A.; Visualization, M.M., A.R., and A.P.; Supervision, A.R. and P.A.; Project administration, G.C. and P.A.; Funding acquisition, P.A. All authors have read and agreed to the published version of the manuscript.

Funding: This research received no external funding.

Acknowledgments: The authors would like to thank Ivan Notardonato for his help during the sampling campaign.

Conflicts of Interest: The authors declare no conflicts of interest.

References

1. Avino, P.; Capannesi, G.; Rosada, A. Characterization and distribution of mineral content in fine and coarse airborne particle fractions by neutron activation analysis. *Toxicol. Environ. Chem.* **2006**, *88*, 633–647. [CrossRef]
2. Avino, P.; Capannesi, G.; Rosada, A. Heavy metal determination in atmospheric particulate matter by Instrumental Neutron Activation Analysis. *Microchem. J.* **2008**, *88*, 97–106. [CrossRef]
3. Alier, M.; Van Drooge, B.L.; Dall'Osto, M.; Querol, X.; Grimalt, J.; Tauler, R. Source apportionment of submicron organic aerosol at an urban background and a road site in Barcelona (Spain) during SAPUSS. *Atmos. Chem. Phys.* **2013**, *20*, 10353–10371. [CrossRef]
4. Alolayan, M.A.; Brown, K.W.; Evans, J.S.; Bouhamra, W.S.; Koutrakis, P. Source apportionment of fine particles in Kuwait City. *Sci. Total Environ.* **2013**, *448*, 14–25. [CrossRef]
5. Crippa, M.; Canonaco, F.; Slowik, J.G.; El Haddad, I.; Decarlo, P.F.; Mohr, C.; Heringa, M.F.; Chirico, R.; Marchand, N.; Temime-Roussel, B.; et al. Primary and secondary organic aerosol origin by combined gas-particle phase source apportionment. *Atmos. Chem. Phys.* **2013**, *13*, 8411–8426. [CrossRef]
6. Mantas, E.; Remoundaki, E.; Halari, I.; Kassomenos, P.; Theodosi, C.; Hatzikioseyian, A.; Mihalopoulos, N. Mass closure and source apportionment of $PM_{2.5}$ by Positive Matrix Factorization analysis in urban Mediterranean environment. *Atmos. Environ.* **2014**, *94*, 154–163. [CrossRef]
7. Karagulian, F.; Belis, C.A.; Dora, C.F.C.; Prüss-Ustün, A.M.; Bonjour, S.; Adair-Rohani, H.; Amann, M. Contributions to cities' ambient particulate matter (PM): A systematic review of local source contributions at global level. *Atmos. Environ.* **2015**, *120*, 475–483. [CrossRef]
8. Manigrasso, M.; Febo, A.; Guglielmi, F.; Ciambottini, V.; Avino, P. Relevance of aerosol size spectrum analysis as support to qualitative source apportionment studies. *Environ. Pollut.* **2012**, *170*, 43–51. [CrossRef]
9. Marini, S.; Buonanno, G.; Stabile, L.; Avino, P. A benchmark for numerical scheme validation of airborne particle exposure in street canyons. *Environ. Sci. Pollut. Res.* **2015**, *22*, 2051–2063. [CrossRef]

10. Neuwahl, F.; Cusano, G.; Gómez Benavides, J.; Holbrook, S.; Roudier, S. *Best Available Techniques (BAT) Reference Document for Waste Incineration*; EUR 29971 EN; Publications Office of the European Union: Luxembourg, 2019. Available online: https://eippcb.jrc.ec.europa.eu/sites/default/files/2020-01/JRC118637_WI_Bref_2019_published_0.pdf (accessed on 10 February 2020). [CrossRef]
11. Eurostat Statistical Books. *Environmental Statistics and Accounts in Europe 2010*; European Union: Strasbourg, France, 2010. Available online: https://ec.europa.eu/eurostat/documents/3217494/5723037/KS-32-10-283-EN.PDF/22a4889d-e6c9-4583-8d17-fb5104e7eec0 (accessed on 13 February 2020).
12. European Commission. *Review of the Thematic Strategy on the Prevention and Recycling of Waste*; Commission Staff Working Document; European Commission: Brussels, Belgium, 2019. Available online: https://ec.europa.eu/environment/waste/strategy.htm (accessed on 20 January 2020).
13. European Commission. Council Directive 2008/98/EC of 19 November 2008. Directive on waste and repealing certain Directives. *Off. J. Eur. Union* **2008**, *L312*, 3–30.
14. Cass, G.R.; Hughes, L.A.; Bhave, P.; Kleeman, M.J.; Allen, J.O.; Salmon, L.G. The chemical composition of atmospheric ultrafine particles. *Philos. Trans. R. Soc. Lond. Ser. A* **2000**, *358*, 2581–2592. [CrossRef]
15. Ranzi, A.; Fustinoni, S.; Erspamer, L.; Campo, L.; Gatti, M.G.; Bechtold, P.; Bonassi, S.; Trenti, T.; Goldoni, C.A.; Bertazzi, P.A.; et al. Biomonitoring of the general population living near a modern solid waste incinerator: A pilot study in Modena, Italy. *Environ. Int.* **2013**, *61*, 88–97. [CrossRef] [PubMed]
16. Allsopp, M.; Costner, P.; Johnston, P. Incineration and human health: State of knowledge of the impacts of waste incinerators on human health (executive summary). *Environ. Sci. Pollut. Res.* **2011**, *8*, 141–145. [CrossRef] [PubMed]
17. Ranzi, A.; Fano, V.; Erspamer, L.; Lauriola, P.; Perucci, C.A.; Forastiere, F. Mortality and morbidity among people living close to incinerators: A cohort study based on dispersion modeling for exposure assessment. *Environ. Health* **2011**, *10*, 22. [CrossRef] [PubMed]
18. Forastiere, F.; Badaloni, C.; De Hoogh, K.; von Kraus, M.K.; Martuzzi, M.; Mitis, F.; Palkovicova, L.; Porta, D.; Preiss, P.; Ranzi, A.; et al. Health impact assessment of waste management facilities in three European countries. *Environ. Health* **2011**, *10*, 53. [CrossRef]
19. Cordioli, M.; Vincenzi, S.; De Leo, G.A. Effects of heat recovery for district heating on waste incineration health impact: A simulation study in Northern Italy. *Sci. Total Environ.* **2013**, *444*, 369–380. [CrossRef]
20. Cordioli, M.; Ranzi, A.; De Leo, G.A.; Lauriola, P. A review of exposure assessment methods in epidemiological studies on incinerators. *J. Environ. Public Health* **2013**, *2013*, 129470. [CrossRef]
21. Lee, C.C.; Huffman, G.L.; Oberacker, D.A. An overview of hazardous/toxic waste incineration. *J. Air Pollut. Control Assoc.* **1986**, *36*, 922–931. [CrossRef]
22. Oppelt, E.T. Incineration of hazardous waste. *JAPCA* **1987**, *37*, 558–586. [CrossRef]
23. USNRC. *Waste Incineration and Public Health*; Committee on Health Effects of Waste Incineration, Ed.; National Academy Press: Washington, DC, USA, 2000; Available online: https://www.nap.edu/catalog/5803/waste-incineration-and-public-health (accessed on 10 February 2020).
24. Chen, Z.; Lin, X.; Lu, S.; Li, X.; Qiu, Q.; Wu, A.; Ding, J.; Yan, J. Formation pathways of PCDD/Fs during the co-combustion of municipal solid waste and coal. *Chemosphere* **2018**, *20*, 862–870. [CrossRef]
25. Wang, G.; Deng, J.; Ma, Z.; Hao, J.; Jiang, J. Characteristics of filterable and condensable particulate matter emitted from two waste incineration power plants in China. *Sci. Total Environ.* **2018**, *639*, 695–704. [CrossRef] [PubMed]
26. Buonanno, G.; Stabile, L.; Avino, P.; Vanoli, R. Dimensional and chemical characterization of particles at a downwind receptor site of a waste-to-energy plant. *Waste Manag.* **2010**, *30*, 1325–1333. [CrossRef] [PubMed]
27. Buonanno, G.; Stabile, L.; Avino, P.; Belluso, E. Chemical, dimensional and morphological ultrafine particle characterization from a waste-to-energy plant. *Waste Manag.* **2011**, *31*, 2253–2262. [CrossRef] [PubMed]
28. Nielsen, M.; Illerup, J.B. Emissionsfaktorer og Emissionsopgørelse for Decentral Kraftvarme, Eltra PSO Projekt 3141, Kortlægning Af Emissionsfaktorer Fra Decentral kraftvarme, Delrapport 6, 2003, nr. 442. Available online: http://www2.dmu.dk/1_viden/2_Publikationer/3_fagrapporter/rapporter/FR442.pdf (accessed on 20 January 2020).
29. Nielsen, M.; Illerup, J.B.; Fogh, C.L.; Johansen, L.P. *PM Emission from CHP Plants < 25MWe*; National Environmental Research Institute of Denmark: Roskilde, Denmark, 2006. Available online: http://www2.dmu.dk/1_Viden/2_Miljoe-tilstand/3_luft/4_adaei/doc/Poster_Eltra_PM.doc (accessed on 20 January 2020).

30. Capannesi, G.; Rosada, A.; Avino, P. Elemental characterization of impurities at trace and ultra-trace levels in metallurgical lead samples by INAA. *Microchem. J.* **2009**, *93*, 188–194. [CrossRef]
31. Avino, P.; Capannesi, G.; Manigrasso, M.; Sabbioni, E.; Rosada, A. Element assessment in whole blood, serum and urine of three Italian healthy sub-populations by INAA. *Microchem. J.* **2011**, *99*, 548–555. [CrossRef]
32. Avino, P.; Capannesi, G.; Renzi, L.; Rosada, A. Instrumental neutron activation analysis and statistical approach for determining baseline values of essential and toxic elements in hairs of high school students. *Ecotoxicol. Environ. Saf.* **2013**, *92*, 206–214. [CrossRef]
33. EN 12341. *Determination of the PM10 Fraction of Suspended Particulate Matter-Reference Method and Field Test Procedure to Demonstrate Reference Equivalence of Measurement Methods*; European Commission: Strasbourg, France, 1988.
34. Erdtmann, G.; Soyka, W. *The Gamma Rays of the Radionuclides*; Wiley-VCH: New York, NY, USA, 1988.
35. Campanella, L.; Crescentini, G.; Avino, P.; Moauro, A. Determination of macrominerals and trace elements in the alga Spirulina platensis. *Analusis* **1998**, *26*, 210–214. [CrossRef]
36. Avino, P.; Carconi, P.; Lepore, L.; Moauro, A. Nutritional and environmental properties of algal products used in healthy diet by INAA and ICP-AES. *J. Radioanal. Nucl. Chem.* **2000**, *244*, 247–252. [CrossRef]
37. Seccaroni, C.; Volante, N.; Rosada, A.; Ambrosone, L.; Bufalo, G.; Avino, P. Identification of provenance of obsidian samples analyzing elemental composition by INAA. *J. Radioanal. Nucl. Chem.* **2008**, *278*, 277–282. [CrossRef]
38. Djingova, R.; Kuleff, I. Instrumental techniques for trace analysis. In *Trace Metals in the Environment*; Markert, B., Friese, K., Eds.; Elsevier: Amsterdam, The Netherlands, 2000; pp. 137–185.
39. Smodiš, B.; Bleise, A. IAEA quality control study on determining trace elements in biological matrices for air pollution research. *J. Radioanal. Nucl. Chem.* **2007**, *271*, 269–274. [CrossRef]
40. European Union. Council Directive 2008/50/EC of 21 May 2008. Directive on ambient air quality and cleaner air for Europe. *Off. J. Eur. Union* **2008**, *L152*, 1–44.
41. Roemer, W.H.; van Wijnen, J.H. Differences among black smoke, PM10, and PM1.0 levels at urban measurement sites. *Environ. Health Perspect.* **2001**, *109*, 51–154.
42. Pérez, N.; Pey, J.; Querol, X.; Alastuey, A.; Lòpez, J.M.; Viana, M. Partitioning of major and trace components in PM_{10}-$PM_{2.5}$-PM_1 at an urban site in Southern Europe. *Atmos. Environ.* **2008**, *42*, 1677–1691. [CrossRef]
43. Vecchi, R.; Marcazzan, G.; Valli, G.; Ceriani, M.; Antoniazzi, C. The role of atmospheric dispersion in the seasonal variation of PM_1 and $PM_{2.5}$ concentration and composition in the urban area of Milan (Italy). *Atmos. Environ.* **2004**, *38*, 4437–4446. [CrossRef]
44. Pakkanen, T.A.; Kerminen, V.-M.; Loukkola, K.; Hillamo, R.E.; Aarnio, P.; Koskentalo, T.; Maenhaut, W. Size distributions of mass and chemical components in street-level and rooftop PM1 particles in Helsinki. *Atmos. Environ.* **2003**, *37*, 1673–1690. [CrossRef]
45. Spindler, G.; Muller, K.; Bruggemann, E.; Gnauk, T.; Herrmann, H. Long-term size-segregated characterization of PM_{10}, $PM_{2.5}$, and PM_1 at the IfT research station Melpitz downwind of Leipzig (Germany) using high and low-volume filter samplers. *Atmos. Environ.* **2004**, *38*, 5333–5347. [CrossRef]
46. Bathmanabhan, S.; Madanayak, S.N.S. Analysis and interpretation of particulate matter-PM_{10}, $PM_{2.5}$ and PM_1 emissions from the heterogeneous traffic near an urban roadway. *Atmos. Pollut. Res.* **2010**, *1*, 184–194.
47. Moauro, A.; Carconi, P.L. A European intercomparison of vegetal standard reference materials, based on INAA and some non nuclear spectrochemical techniques. *J. Radioanal. Nucl. Chem.* **1991**, *151*, 149–157. [CrossRef]
48. World Health Organization. *Environmental Health Criteria 224: Arsenic and Arsenic Compounds*; WHO: Geneva, Switzerland, 2001. Available online: https://www.who.int/ipcs/publications/ehc/ehc_224/en/ (accessed on 16 February 2020).
49. Avino, P.; Capannesi, G.; Rosada, A. Source identification of inorganic airborne particle fraction (PM_{10}) at ultratrace levels by means of INAA short irradiation. *Environ. Sci. Pollut. Res.* **2014**, *21*, 4527–4538. [CrossRef]
50. IARC. *Monographs on the Evaluation of the Carcinogenic Risk of Chemicals to Humans: Chromium and Chromium Compounds*; IARC: Lyon, France, 1990; Volume 49. Available online: http://publications.iarc.fr/67 (accessed on 3 February 2020).
51. Besso, A.; Nyberg, F.; Pershagen, G. Air pollution and lung cancer mortality in the vicinity of a non ferrous metal smelters in Sweden. *Int. J. Cancer* **2003**, *107*, 4448–4452. [CrossRef]

52. Guzzi, G.; Colombo, A.; Girardi, F.; Pietra, R.; Rossi, G.; Toussaint, N. Comparison of various analytical techniques for homogeneity test of candidate standard reference materials. *J. Radioanal. Nucl. Chem.* **1977**, *39*, 263–276. [CrossRef]
53. Beijer, K.; Jernelöv, A. Sources, transport and transformation of metals in the environment. In *Handbook on the Toxicology of Metals*, 2nd ed.; Frindberg, L., Nordberg, G.F., Vouk, V.B., Eds.; Elsevier: Amsterdam, The Netherlands, 1986; Volume 3, pp. 68–74.
54. Mari, M.; Nadal, M.; Schuhmacher, M.; Domingo, J.L. Exposure to heavy metals and PCDD/Fs by the population living in the vicinity of a hazardous waste landfill in Catalonia, Spain: Health risk assessment. *Environ. Int.* **2009**, *35*, 1034–1039. [CrossRef] [PubMed]
55. Chen, J.; Tan, M.; Li, Y.; Zheng, J.; Zhang, Y.; Shan, Z.; Zhang, G.; Li, Y. Characteristics of trace elements and lead isotope ratios in $PM_{2.5}$ from four sites in Shanghai. *J. Hazard. Mater.* **2008**, *156*, 36–43. [CrossRef] [PubMed]
56. Talbi, A.; Kerchich, Y.; Kerbachi, R.; Boughedaoui, M. Assessment of annual air pollution levels with PM_1, $PM_{2.5}$, PM_{10} and associated heavy metals in Algiers, Algeria. *Environ. Pollut.* **2018**, *232*, 252–263. [CrossRef]
57. Rudnick, R.L.; Gao, S. Composition of the continental crust. In *Treatise on Geochemistry*; Holland, H.D., Turekian, K.K., Eds.; Elsevier: Amsterdam, The Netherlands, 2003; Volume 3, pp. 1–64.
58. Misaelides, P.; Samara, C.; Noli, F.; Kouimtzis, T.; Anou, I. Toxic element concentrations in airborne particulate matter in the area of Thessaloniki, Greece. *Sci. Total Environ.* **1993**, *130*, 139–146. [CrossRef]
59. Bergamaschi, L.; Rizzio, E.; Valcuvia, M.G.; Verza, G.; Profumo, A.; Gallorini, M. Determination of trace elements and evaluation of their enrichment factors in *Himalayan lichens*. *Environ. Pollut.* **2002**, *120*, 137–144. [CrossRef]
60. Aspinall, A.; Feather, S.W.; Renfrew, C. Neutron Activation Analysis of Aegean obsidians. *Nature* **1972**, *237*, 333–334. [CrossRef]
61. Escofier, B.; Pagès, J. *Analyses Factorielles Multiples*; Dunod: Paris, France, 1988.
62. Hohnson, R.A.; Wichern, D.W. *Applied Multivariate Statistical Analysis*; Prentice-Hill: Upper Saddle River, NJ, USA, 2002.
63. Tanagra. Available online: http://eric.univ-lyon2.fr/~{}ricco/tanagra/en/tanagra.html (accessed on 14 January 2020).
64. Jain, A.K.; Dubes, R.C. *Algorithms for Clustering Data*; Prentice Hall: Upper Saddle River, NJ, USA, 1988.
65. Tibshirani, R.; Walther, G.; Hastie, T. Estimating the number of clusters in a dataset via the gap statistics. *J. R. Stat. Soc. Ser. B* **2001**, *63*, 411–423. [CrossRef]
66. Febo, A.; Guglielmi, F.; Manigrasso, M.; Ciambottini, V.; Avino, P. Local air pollution and long–range mass transport of atmospheric particulate matter: A comparative study of the temporal evolution of the aerosol size fractions. *Atmos. Pollut. Res.* **2010**, *1*, 141–146. [CrossRef]